CHEMISTRY
A EUROPEAN JOURNAL

DOI: 10.1002/chem.200800188

Ultrafast Excited State Dynamics Controlling Photochemical Isomerization of *N*-Methyl-4-[*trans*-2-(4-pyridyl)ethenyl]pyridinium Coordinated to a {$Re^{I}(CO)_3$(2,2′-bipyridine)} Chromophore

Michael Busby,[a] František Hartl,[b] Pavel Matousek,[c] Mike Towrie,[c] and Antonín Vlček, Jr.*[a]

Abstract: Two multifunctional photoactive complexes $[Re(Cl)(CO)_3(MeDpe^+)_2]^{2+}$ and $[Re(MeDpe^+)(CO)_3(bpy)]^{2+}$ ($MeDpe^+$ = *N*-methyl-4-[*trans*-2-(4-pyridyl)ethenyl]pyridinium, bpy = 2,2′-bipyridine) were synthesized, characterized, and their redox and photonic properties were investigated by cyclic voltammetry; ultraviolet–visible–infrared (UV/Vis/IR) spectroelectrochemistry, stationary UV/Vis and resonance Raman spectroscopy; photolysis; picosecond time-resolved absorption spectroscopy in the visible and infrared regions; and time-resolved resonance Raman spectroscopy. The first reduction step of either complex occurs at about −1.1 V versus Fc/Fc^+ and is localized at $MeDpe^+$. Reduction alone does not induce a *trans*→*cis* isomerization of $MeDpe^+$. $[Re(Cl)(CO)_3(MeDpe^+)_2]^{2+}$ is photostable, while $[Re(MeDpe^+)(CO)_3(bpy)]^{2+}$ and free $MeDpe^+$ isomerize under near-UV irradiation. The lowest excited state of $[Re(Cl)(CO)_3(MeDpe^+)_2]^{2+}$ has been identified as the $Re(Cl)(CO)_3 \rightarrow MeDpe^+$ ^{3}MLCT (MLCT = metal-to-ligand charge transfer), decaying directly to the ground state with lifetimes of ≈42 (73%) and ≈430 ps (27%). Optical excitation of $[Re(MeDpe^+)(CO)_3(bpy)]^{2+}$ leads to population of $Re(CO)_3 \rightarrow MeDpe^+$ and $Re(CO)_3 \rightarrow$bpy ^{3}MLCT states, from which a $MeDpe^+$ localized intraligand $^3\pi\pi^*$ excited state (^{3}IL) is populated with lifetimes of ≈0.6 and ≈10 ps, respectively. The ^{3}IL state undergoes a ≈21 ps internal rotation, which eventually produces the *cis* isomer on a much longer timescale. The different excited-state behavior of the two complexes and the absence of thermodynamically favorable interligand electron transfer in excited $[Re(MeDpe^+)(CO)_3(bpy)]^{2+}$ reflect the fine energetic balance between excited states of different orbital origin, which can be tuned by subtle structural variations. The complex $[Re(MeDpe^+)(CO)_3(bpy)]^{2+}$ emerges as a prototypical, multifunctional species with complementary redox and photonic behavior.

Keywords: charge transfer · chromophores · excited states · isomerization · photochemistry · rhenium

Introduction

Rhenium(I) carbonyl complexes $[Re^{I}(X)(CO)_3(N,N)]^n$ (N,N = chelating polypyridines, α-diimines, X = axial ligand, $n = 0, 1+, 2+$) and $[Re^{I}(Cl)(CO)_3(A)_2]^n$ (A = N-coordinated π-acceptor ligand) combine diverse and tunable photophysics and photochemistry with chemical stability and synthetic flexibility.[1] These chromophores can be attached to proteins, incorporated into conductive polymers and molecular wires, liquid crystals, DNA, or linked with specific substrate binding units either through the axial ligand X or by a judicious modification of the α-diimine ligand. This unique combination of chemical and photonic properties makes Re^{I} carbonyl diimines very promising as functional components of molecular photonic devices.

[a] Dr. M. Busby, Prof. A. Vlček, Jr.
School of Biological and Chemical Sciences
Queen Mary, University of London, Mile End Road
London E1 4NS (UK)
Fax: (+44) 20-7882-7427
E-mail: a.vlcek@qmul.ac.uk

[b] Dr. F. Hartl
Van't Hoff Institute for Molecular Sciences,
University of Amsterdam, Nieuwe Achtergracht 166
1018 WV Amsterdam (The Netherlands)

[c] Dr. P. Matousek, Dr. M. Towrie
Central Laser Facility, Science & Technology Facilities Council
Rutherford Appleton Laboratory, Didcot
Oxfordshire OX11 0QX (UK)

Supporting information for this article is available on the WWW under http://www.chemeurj.org/ or from the author.

The chemical nature and bonding properties of the axial ligand X determine the character of the lowest excited state(s) and, hence, the photochemical and photophysical properties.[1] Usually, the lowest excited state contains a predominant contribution from a $Re(CO)_3 \rightarrow N,N$ metal-to-ligand charge-transfer (MLCT) excitation. This is a typical case of complexes containing an axial ligand X without pronounced π-donating or -accepting properties, such as pyridine derivatives.[1–4] The MLCT character can mix with a $X \rightarrow N,N$ ligand-to-ligand charge transfer (XLCT, also called LLCT), if X is a π donor (NCS^-, halides).[1–3,5–7] Rhenium(I) complexes with MLCT or MLCT/XLCT excited states are photostable and luminescent. Highly delocalized, large polypyridines N,N (some phenanthroline derivatives; dppz = dipyrido[3,2-a:2',3'-c]phenazine) and/or strongly electron-accepting X (isonitriles), introduce low-lying intraligand, IL-(N,N), excited states, which originate in ligand localized ππ* excitation.[1] Re^I carbonyl diimine complexes are mostly photostable and suitable as sensors or switches.[4,8–22] In rare cases,[23,24] some of which will be discussed below, the lowest excited state is localized on the ligand X and isomerization may ensue after its population.

Mixing between excited-state characters, which defies usual textbook classifications, is very common in Re^I complexes. Thus, in addition to the MLCT–XLCT mixing mentioned above, the IL (intraligand) and CT (charge transfer) characters can mix as well.[1–4,25] As their detailed excited-state characters are very sensitive to the medium, Re^I complexes can serve as probes of the character and dynamics of the chromophore environment, which can be varied from simple solvents to polymers or protein binding sites.[4,10]

Optical excitation of the $\{Re^I(CO)_3(N,N)\}$ chromophore into an MLCT excited state redistributes the electron density to $\{Re^{II}(CO)_3(N,N^{\bullet-})\}$. In response, the axial ligand X can perform various chemical functions, depending on whether it is an electron donor, electron acceptor, or an energy acceptor. Thus, for example, reducing ligands X (phenothiazine, tryptophane, tyrosine) can act as electron donors toward the Re^{II} center, effectively quenching the ^{3}MLCT excited state.[18,26–33] Recently, we have investigated the mechanisms of two ultrafast optically induced processes involving the axial ligand X: an interligand electron transfer (ILET)[34,35] in $[Re(MQ^+)(CO)_3(bpy)]^{2+}$ and *trans*→*cis* isomerization in $[Re(stpy)(CO)_3(bpy)]^+$ and $[Re(Cl)(CO)_3(stpy)_2]$, as well as related complexes containing *trans*-phenyl-azopyridine[23,24] (see Figure 1 for formulas and abbreviations of the ligands and complexes). ILET involves an electron transfer from the $bpy^{\bullet-}$ ligand in the ^{3}MLCT excited state to the electron-accepting MQ^+ ligand, which occurs with a lifetime of about 8 ps. The *trans*→*cis* isomerization of coordinated stpy has been shown to take place from a ^{3}IL excited state localized at the stpy ligand, which is populated from a $Re(CO)_3 \rightarrow bpy$ ^{3}MLCT state by ultrafast (3.5 ps), intramolecular energy transfer. This kind of "intramolecular sensitization" of intraligand photochemistry by MLCT excitation,[13,36–41] the kinetics of which were first determined[23] for $[Re(stpy)(CO)_3(bpy)]^+$, opens interesting possibilities in designing new molecular photonic switches and sensors.[11]

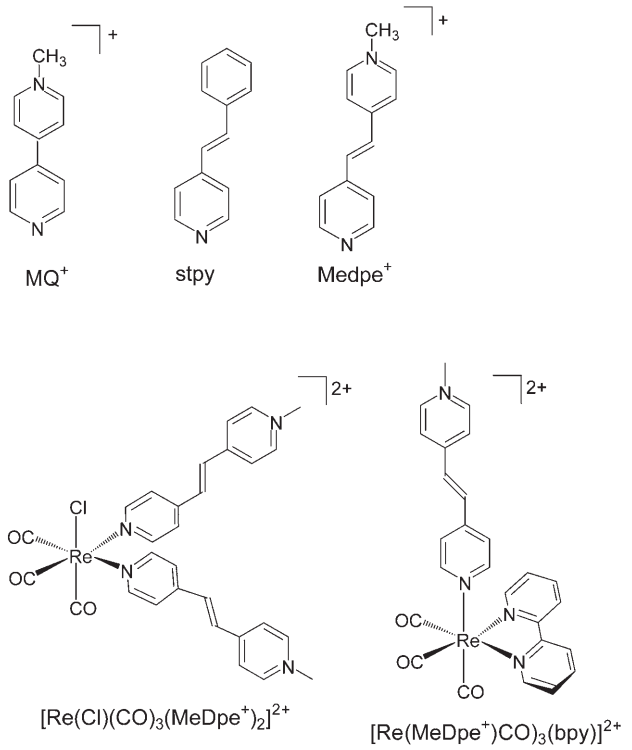

Figure 1. Schematic structures of the ligands and the complexes $[Re(Cl)(CO)_3(MeDpe^+)_2]^{2+}$ and $[Re(MeDpe^+)(CO)_3(bpy)]^{2+}$. MQ^+ = *N*-methyl-4,4′-bipyridinium (MQ^+), stpy = *trans*-4-styryl-pyridine, $MeDpe^+$ = *N*-methyl-4-[*trans*-2-(4-pyridyl)ethenyl]pyridinium, bpy = 2,2′-bipyridine. The prefix "*trans*-" is hereinafter omitted for brevity. Metal-to-ligand charge transfer directed to $MeDpe^+$ or bpy will be denoted as MLCT($MeDpe^+$) or MLCT(bpy), respectively.

Herein, we introduce these photoreactive properties in two new complexes $[Re(Cl)(CO)_3(MeDpe^+)_2]^{2+}$ and $[Re(MeDpe^+)(CO)_3(bpy)]$ (Figure 1) and investigate their redox properties, photochemistry, and excited-state dynamics. The excited complexes may undergo a *trans*→*cis* isomerization of the C=C bond, ILET with the oxidizing methylpyridinium ring, or just a simple radiative or nonradiative decay to the ground state, raising important questions about the factors controlling the photonic behavior of these multifunctional chromophores.

Results

Redox properties: electrochemistry and spectroelectrochemistry: The cyclic voltammogram of free $MeDpe^+$ in THF shows a sharp (i.e., electrochemically reversible) cathodic peak at $E_{p,c} = -1.31$ V versus Fc/Fc^+. No anodic counter peak was observed at a 100 $mV\,s^{-1}$ scan rate. Reduction is chemically irreversible due to fast inactivation of its primary product, $MeDpe^{\bullet}$, presumably by dimerization or oligomerization. A weak, broad, anodic peak at −0.18 V is observed on the reversed scan. A second reduction of

$MeDpe^+$ occurs at −1.94 V as a weak, broad, chemically irreversible peak.

The complex $[Re(Cl)(CO)_3(MeDpe^+)_2]^{2+}$ in acetonitrile (MeCN) has a single two-electron wave at $E_{1/2} = -1.08$ V ($\Delta E_p = 80$ mV) with a peak-current ratio $I_{p,a}/I_{p,c} = 0.67$ at $v = 100\ mV\,s^{-1}$ at room temperature attributed to simultaneous reduction of both $MeDpe^+$ ligands to $MeDpe^{\bullet}$. Coordination to Re partially stabilizes the $MeDpe^{\bullet}$ radical. However, the anodic counter-peak disappears on lowering the temperature or decreasing the scan rate to $2\ mV\,s^{-1}$ when using a thin-layer spectroelectrochemical cell.

The infrared (IR) spectrum of $[Re(Cl)(CO)_3(MeDpe^+)_2]^{2+}$ in butyronitrile (PrCN) at room temperature exhibits three ν(CO) bands at 2024, 1921, and 1892 cm^{-1}. Scanning the potential over the whole irreversible cathodic wave shifts the ν(CO) bands only slightly to 2021, 1915, and 1887 cm^{-1}. Both $MeDpe^+$ ligands are reduced in this step, as revealed by the complete disappearance of the bands at 1647 and 1636 cm^{-1}, some of which belong[42] to the ν(C=C)/δ(CH) vibration. At the same time, a new unresolved band grows in at 1666 cm^{-1}. The small downward shift of ν(CO) indicates that the reduction is predominantly localized at $MeDpe^+$, being largely electronically decoupled from the $Re(CO)_3$ moiety. Ultraviolet-visible (UV/Vis) spectra measured in THF during reduction show only very weak features due to the pyridinyl radical unit at 506, 593, 693, and 765 nm, with an isosbestic point at 455 nm. The low intensity of these bands suggests that most of the $[Re(Cl)(CO)_3(MeDpe^{\bullet})_2]$ reduction product is converted to a species that does not have a radical character.

$[Re(MeDpe^+)(CO)_3(bpy)]^{2+}$ in THF at room temperature exhibits three reversible cathodic waves at $E_{1/2} = -1.15$ ($\Delta E_p = 70$ mV), −1.53 ($\Delta E_p = 70$ mV) and −1.76 V ($\Delta E_p = 80$ mV), Figure 2 top. Similar results were obtained in acetonitrile and in butyronitrile, in which the potentials of the cathodic waves are slightly less negative: −1.08, −1.49 and −1.69 V. The first reduction is assigned to the $MeDpe^+/MeDpe^{\bullet}$ ligand localized couple, based on the similarity with the potentials of the $[Re(Cl)(CO)_3(MeDpe^+)_2]^{2+}$ and $MeDpe^+$ reductions. The second reduction is attributed to the bpy ligand, because it occurs at a potential very close to that of the bpy localized reduction in $[Re(MQ^+)(CO)_3(bpy)]^+$, −1.57 V.[43] This assignment was confirmed spectroelectrochemically, see below. The third, most negative, step is attributed to the second MeDpe localized reduction, based on comparison with the cyclic voltammetry (CV) of the free ligand.

The first reduction step of $[Re(MeDpe^+)(CO)_3(bpy)]^{2+}$ becomes chemically irreversible in THF on decreasing the temperature to 208 K (Figure 2 bottom) or slowing the scan rate in a thin-layer spectroelectrochemical cell to $2\ mV\,s^{-1}$. The sharp cathodic wave lies at $E_{p,c} = -1.22$ V (THF, 208 K) and the reverse scan shows a very weak counter peak at a slightly more positive potential. A more prominent, broad anodic counter-peak occurs at $E_{p,a} = -0.17$ V, similar to the free $MeDpe^+$. The second cathodic process, at $E_{1/2} = -1.60$ V, remains electrochemically reversible ($\Delta E_p =$ 80 mV), but becomes only partly reversible chemically ($I_{p,a}/I_{p,c} = 0.76$ at $v = 100\ mV\,s^{-1}$). The reverse anodic scan triggered beyond this wave reveals a new, small anodic wave at $E_{p,a} = -1.49$ V. The potential and shape of the third cathodic process remain unaffected by the temperature change: $E_{1/2} = -1.76$ V ($\Delta E_p = 80$ mV). However, the corresponding peak current is much smaller than of the two preceding steps. Qualitatively identical temperature dependence of the cyclovoltammetric response of $[Re(MeDpe^+)(CO)_3(bpy)]^{2+}$ was encountered in acetonitrile (233 K) and butyronitrile (208 K).

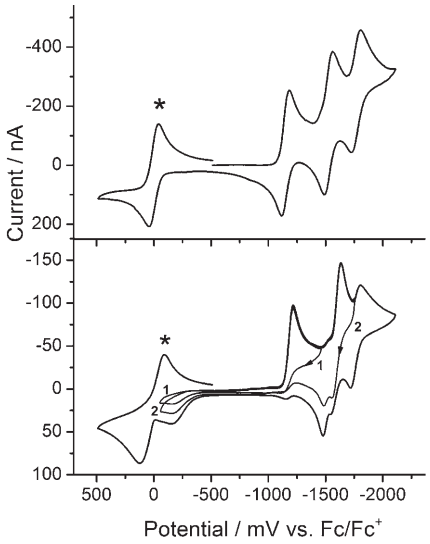

Figure 2. Cyclic voltammetry of $[Re(MeDpe^+)(CO)_3(bpy)]^{2+}$ in THF, scan rate $100\ mV\,s^{-1}$. Top: room temperature, bottom at 208 K. The curves marked 1 and 2 show CVs with the potential scan reversed beyond the first and second reduction peaks, respectively. Ferrocene was added as an internal potential and reversibility standard, marked by an asterisk.

IR spectroelectrochemistry of $[Re(MeDpe^+)(CO)_3(bpy)]^{2+}$ in THF at room temperature shows that the first one-electron reduction results only in a very small shift of the two ν(CO) bands from 2035 and 1929 (broad) to 2032.5 and 1926 cm^{-1} (broad), respectively. This negligible ν(CO) spectral change indicates that the Re→CO π back-donation is essentially unaffected, providing evidence for localization of the first reduction at the remote pyridinium part of $MeDpe^+$. Reduction of $MeDpe^+$ in $[Re(MeDpe^+)(CO)_3(bpy)]$ also leads to the disappearance of weak absorption bands at 1615, 1647, and 1636 cm^{-1}, which is accompanied by the growth of new bands at 1666 and 1600 cm^{-1}. Reoxidation of the one-electron-reduced complex at potentials about 1 V less results in shifting ν(CO) bands back to 2034 and 1929 cm^{-1}. The original $MeDpe^+$ bands at 1647 and 1636 are not recovered by reoxidation, although the bands of the reduced species at 1666 and 1600 cm^{-1} disappear completely. These observations are in line with the irreversible character of the $MeDpe^+$ reduction and show that chemical reactions of the electrochemically produced $[Re(MeDpe^{\bullet})(CO)_3(bpy)]^+$ concern the MeDpe C=C bond.

They cannot be attributed to *trans*→*cis* isomerization, for which a recovery of stretching vibrations after reoxidation is expected. Isomerization of MeDpe$^{\bullet}$ can also be excluded based on comparison with the chemistry of analogous radicals.[44] Dimerization or oligomerization of the radical ligand thus remains likely candidates for the secondary reactions of the electrochemically produced radicals.

The second reduction of $[Re(MeDpe^{+})(CO)_3(bpy)]^{2+}$ is accompanied by chemical decomposition, which leads to three products characterized by A′(1) ν(CO) bands at 2014, 2007.5, and 2002.5 cm^{-1}. At later stages of the reduction, the IR spectrum becomes dominated by bands at 2007.5, 1899, and 1892 cm^{-1}, which belong to a species in which the bpy ligand is reduced to bpy$^{\bullet-}$, again in agreement with the cyclic voltammetry. For comparison, ν(CO) bands of $[Re(MQ^{\bullet})(CO)_3(bpy^{\bullet-})]$ occur[43] at 2003 and 1892 cm^{-1} (br). IR spectroelectrochemistry of $[Re(MeDpe^{+})(CO)_3(bpy)]^{2+}$ in MeCN at room temperature and in PrCN at 253 K gives essentially the same results. The ν(CO) bands shift upon the first MeDpe^{+} localized reduction by 1–1.5 cm^{-1} at 253 K.

UV/Vis spectra recorded in situ during the first reduction of $[Re(MeDpe^{+})(CO)_3(bpy)]^{2+}$ in THF in the optically transparent thin-layer electrochemical (OTTLE) cell at room temperature show a strong absorbance decrease in the ultraviolet (UV) region and growth of new bands characteristic of the pyridinyl radical unit at 515, 596, 710, and 780 nm, with an isosbestic point at 402 nm (Figure 3). The last two bands gradually shift to 697 and 767 nm, respectively, in the course of the reduction, presumably reflecting a secondary reaction of the reduced product. UV/Vis spectra show no signs of the characteristic spectral features[45–48] of bpy$^{\bullet-}$, in accord with the MeDpe localization of the first reduction.

The counterintuitive loss of chemical reversibility of the first reduction wave at low temperatures, observed for both $[Re(Cl)(CO)_3(MeDpe^{+})_2]^{2+}$ and $[Re(MeDpe^{+})(CO)_3(bpy)]^{2+}$ (A), indicates that the primary electrochemical products, $[Re(Cl)(CO)_3(MeDpe^{\bullet})_2]$ and $[Re(MeDpe^{\bullet})(CO)_3(bpy)]^{+}$ (B) are in a temperature-dependent equilibrium $A \overset{\pm e^-}{\leftrightarrow} B \overset{1}{\rightleftarrows} C \overset{3}{\rightarrow} D$ with another species ($\overset{2}{C}$) that undergoes further irreversible chemical reaction to the product (D). The intermediate C is reoxidized at a potential that is only a little more positive than that of the first reduction wave of A, while reoxidation of D is shifted much more positively to about −0.17 V. Based on the spectroelectrochemical results, we can conclude that:

1) The chemical transformations 1, 2, and 3 concern the MeDpe$^{\bullet}$ ligand, in particular the C=C bond. However, they cannot be attributed to *trans*→*cis* isomerization.
2) The pyridinyl radical chromophore is preserved in C but not in D.
3) Reoxidation of neither C nor D regenerates the starting complex A.
4) The irreversible transformation 3 is more prominent in the case of $[Re(Cl)(CO)_3(MeDpe^{+})_2]^{2+}$, possibly due to the presence of two MeDpe$^{\bullet}$ radicals in B. Identification of the products will be the subject of further research.

UV/Vis and resonance Raman spectra: A UV/Vis absorption spectrum (Figure 4a) of MeDpe^{+} in MeCN exhibits an intense absorption band at 316 nm (ε_{max} = 28400 M^{-1} cm^{-1}) with a weak shoulder at about 330 nm. Upon complexation to $[Re(Cl)(CO)_3(MeDpe^{+})_2]^{2+}$, the band shifts slightly to 307 nm (ε_{max} = 47200 M^{-1} cm^{-1}) and a pronounced shoulder emerges at about 340 nm (ε = 31500 M^{-1} cm^{-1}), with a "tail"

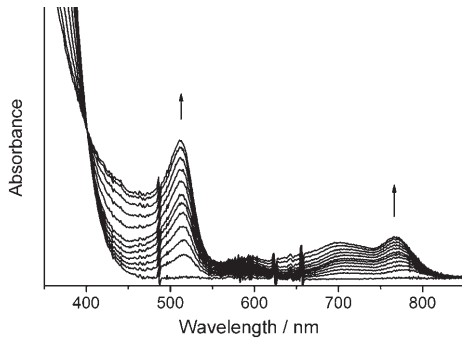

Figure 3. UV/Vis spectroelectrochemistry of $[Re(MeDpe^{+})(CO)_3(bpy)]^{2+}$ in THF at room temperature. Spectra monitored during reduction between −1.10 and −1.35 V versus Fc/Fc^{+} evolve in the direction of the arrows.

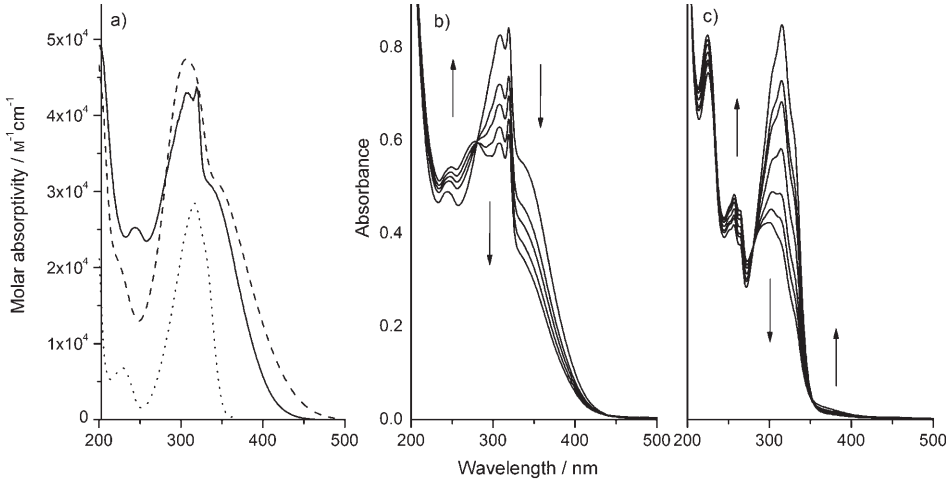

Figure 4. a) UV/Vis absorption spectra of MeDpe^{+} (dotted), $[Re(Cl)(CO)_3(MeDpe^{+})_2]^{2+}$ (dashed), and $[Re(MeDpe^{+})(CO)_3(bpy)]^{2+}$ (solid). b) Photoisomerization of $[Re(MeDpe^{+})(CO)_3(bpy)]^{2+}$ under 365 nm irradiation. c) Photoisomerization of MeDpe^{+} under combined 313+334 nm irradiation. Irradiation intervals about 15 s. All measurements in MeCN.

extending to ≈480 nm. $[Re(MeDpe^+)(CO)_3(bpy)]^{2+}$ shows spectral features similar to those of $[Re(Cl)(CO)_3(MeDpe^+)_2]^{2+}$: an intense band at 307 nm (ε_{max} = 42900 м$^{-1}$ cm^{-1}) with a shoulder at 335 nm (ε_{max} = 30100 м$^{-1}$ cm^{-1}), and a sharp spike at 319 nm that is typical for bpy. The large molar absorption of the main UV band of $MeDpe^+$ and its complexes is indicative of a $\pi\rightarrow\pi^*$ IL character. The "tail" that extends in the spectra of the complexes beyond 400 nm could originate in MLCT transition(s). Neither of the complexes is luminescent in MeCN under 400 nm excitation.

Resonance Raman (rR) spectroscopy provides further information about the character of the electronic transitions by identifying coupled molecular vibrations. The rR spectra of both complexes (Figure 5 top) were recorded in acetonitrile and were excited at 457.9 nm, into the "tail" of the lowest energy absorption band. The spectrum of $[Re(Cl)(CO)_3(MeDpe^+)_2]^{2+}$ shows a medium intensity band due to the in-phase A′(1) ν(CO) carbonyl mode at 2027 cm^{-1}. The strongest band occurs at 1634 cm^{-1} with a shoulder at 1619 cm^{-1}. It is assigned to a coupled ν(C=C)/δ(C–H) vibration of the ethylenic group of the $MeDpe^+$ ligand.[23,42] Less intense bands due to $MeDpe^+$ vibrations are observed at 1220, 1212, 1188, and 1027 cm^{-1}. The band at 1220/1212 cm^{-1} is absent in rR spectra of analogous stpy complexes, while a similar band occurs in the spectrum of $[Re(MQ^+)(CO)_3(bpy)]^{2+}$ and is assigned[49] to a $\nu(N^+–CH_3)$ vibration. Observation of enhanced bands due to $MeDpe^+$ vibrations is compatible with both MLCT and IL characters of the resonant electronic transitions, while enhancement of the ν(CO) band is diagnostic[7,42,50–53] of $Re(CO)_3\rightarrow MeDpe^+$ MLCT. By combining information from UV/Vis and rR spectroscopy, we may conclude that the lowest near-UV absorption band is primarily due to an IL transition while the "tail" extending into the visible region originates in an MLCT transition from $Re(Cl)(CO)_3$ to $MeDpe^+$.

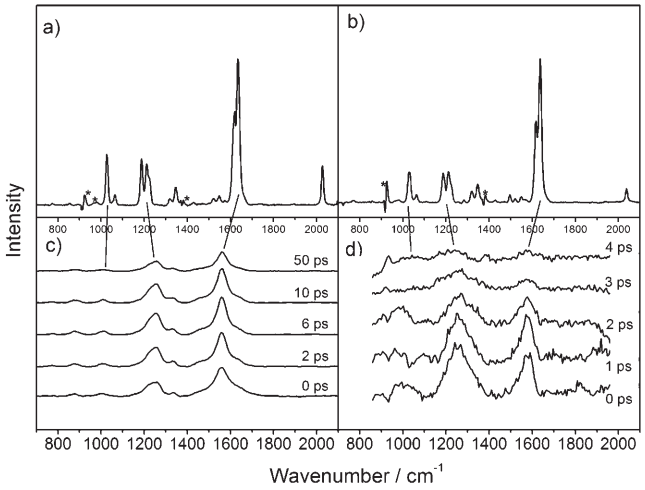

Figure 5. Stationary resonance Raman (rR) and time-resolved resonance Raman (TR^3) spectra of $[Re(Cl)(CO)_3(MeDpe^+)_2]^{2+}$ (left) and $[Re(MeDpe^+)(CO)_3(bpy)]$ (right) in MeCN. Top: rR spectra of a) $[Re(Cl)(CO)_3(MeDpe^+)_2]^{2+}$ and b) $[Re(MeDpe)(CO)_3(bpy)]^{2+}$, excited at 457.9 nm. Bottom: Kerr-gate TR^3 spectra of c) $[Re(Cl)(CO)_3(MeDpe^+)_2]^{2+}$, measured with a 510 nm probe at 0, 2, 6, 10, and 50 ps after 400 nm excitation, and d) $[Re(MeDpe^+)(CO)_3(bpy)]^{2+}$ measured with a 525 nm probe at 0, 1, 2, 3, and 4 ps after 400 nm excitation. Baseline corrected for residual emission. Asterisk indicates regions of solvent subtraction.

The rR spectrum of $[Re(MeDpe^+)(CO)_3(bpy)]^{2+}$ (Figure 5) is qualitatively similar to that of $[Re(Cl)(CO)_3(MeDpe^+)_2]$. The most intense band, at 1637 cm^{-1} with a shoulder at 1617 cm^{-1}, is again attributed to the ν(C=C)/δ(CH) vibration of the $MeDpe^+$ ethylenic moiety.[42] Weaker bands due to $MeDpe^+$ vibrations are seen at 1347 (w), 1211 (m, probably $\nu(N^+–CH_3)$), 1187 (m), and 1030 cm^{-1} (m) . The band due to the ν(CO) A′(1) mode is found at 2037 cm^{-1}. However, its intensity relative to the strongest peak, 1637 cm^{-1}, is almost three times lower than in the case of $[Re(Cl)(CO)_3(MeDpe^+)_2]^{2+}$. It follows that the resonance enhancement originates mostly in an IL transition localized on $MeDpe^+$, with a smaller contribution from a $Re(CO)_3\rightarrow MeDpe^+$ MLCT transition. The only feature due to a bpy localized vibration was found at 1497 cm^{-1} (vw), which is too weak to indicate any resonant enhancement originating in a MLCT(bpy) transition.

Photoisomerization: Irradiation of $MeDpe^+$ in MeCN at 313 + 334 nm causes an isosbestic evolution (at 280 nm) of the UV spectrum, in which the band at 316 nm decreases in intensity and a new peak at 248 nm grows (Figure 4c). This spectral change is characteristic of a *trans→cis* photoisomerization, as was demonstrated[54] for an analogous compound *trans*-1,2-bis(1-methyl-4-pyridinium)ethylene (Me_2Dpe^{2+}). A similar isosbestic conversion was observed upon irradiation of $[Re(MeDpe^+)(CO)_3(bpy)]^{2+}$ at 365 nm: intensities of the bands at 315 and 257 nm decreased and grew, respectively, with an isosbestic point at 280 nm (Figure 4b). As with the free ligand, we attribute this spectral change to the *trans→cis* photoisomerization of the $MeDpe^+$ ligand. Thermal regeneration of the *trans* isomer was observed in the dark within a few days for both the ligand and the complex. In contrast, no photoreaction takes place upon irradiation of $[Re(Cl)(CO)_3(MeDpe^+)_2]^{2+}$ at 365 nm.

Transient absorption spectroscopy: The transient absorption (TA) spectrum of $[Re(Cl)(CO)_3(MeDpe^+)_2]^{2+}$ measured after excitation at 400 nm shows intense bands with maxima at 505, 710–720, and beyond 790 nm, and shoulders at ≈660 and 740 nm (Figure 6). Comparison with the TA spectra of the ion-pair CT state[54,55] of $[Me_2dpe^{2+}][I^-]_2$ allows us to assign the TA bands to the reduced $MeDpe^{\bullet}$ ligand in the ^{3}MLCT($MeDpe^+$) excited state, which can be formulated as approximately $[Re^{II}(Cl)(CO)_3(MeDpe^{\bullet})(MeDpe^+)]^{2+}$. The early time evolution of the TA spectra is complicated by relaxation, which is manifested by a dynamic blue shift of the 505 nm band within the first 1 ps from its initial position at ≈522 nm.

Both excited state bands decay with biexponential kinetics, which is, within the experimental accuracy, independent

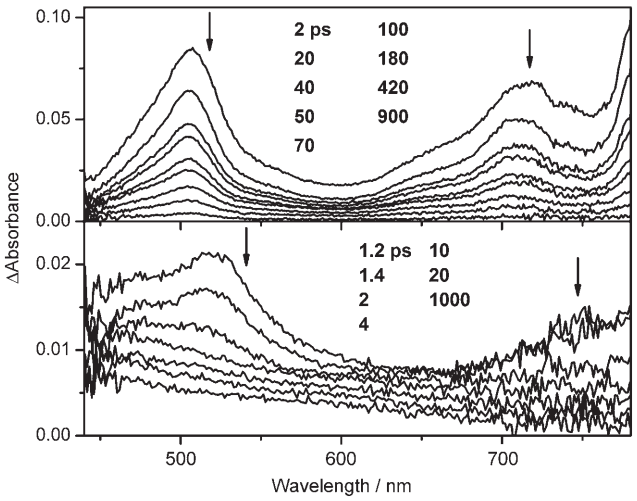

Figure 6. Transient absorption spectra of $[Re(Cl)(CO)_3(MeDpe^+)_2]^{2+}$ (top) and $[Re(MeDpe^+)(CO)_3(bpy)]^{2+}$ (bottom) measured at selected time delays (ps) after 393 nm excitation in MeCN. Chirp distorts early spectral timing between 0–2 ps. The spectra evolve in the direction of the arrows.

of the excitation wavelength. Lifetimes of 37.5 ± 0.5 ps (73%) and 433 ± 20 ps (27%) were determined from the decay of absorbance averaged over the range 499–511 nm. Similar kinetics were found at 710–720 and 784–790 nm. The presence of two parallel decay pathways can be explained by the simultaneous population of two close lying excited states of the same ^{3}MLCT(MeDpe$^+$) character, which differ in the nature of the depopulated dπ(Re) orbital or by two conformations with different orientation of the MeDpe$^+$ ligands. The TA spectra show that both ^{3}MLCT(MeDpe$^+$) states decay directly to the ground state, without any accompanying chemical reaction, in agreement with the photostability of $[Re(Cl)(CO)_3(MeDpe^+)_2]^{2+}$ upon continuous irradiation.

The picosecond TA spectra of $[Re(MeDpe^+)(CO)_3(bpy)]^{2+}$ point to a more complex excited state behavior (Figure 6 bottom). Immediately after excitation, we see two broad weak bands at $\approx$530 nm and between 700–800 nm. In addition, a flat shoulder occurs between 450–475 nm and the absorption extends into the NIR spectral region. Because of their similarity with excited state absorption bands of $[Re(Cl)(CO)_3(MeDpe^+)_2]^{2+}$, the 530 and 700–800 nm bands are attributed to the ^{3}MLCT(MeDpe$^+$) state. A flat absorption between 450–475 nm was seen in the excited state spectra[56–58] of $[Re(Cl)(CO)_3(bpy)]$, $[Re(Etpy)(CO)_3(4,4'\text{-}Me_2\text{-}bpy)]^+$ (Etpy = 4-ethylpyridine) and similar complexes and is attributed to a ^{3}MLCT(bpy) excited state. After 4 ps, these bands disappear, leaving a broad absorption, which stretches across the whole spectrum, monotonically increasing into the UV region. The spectrum remains stationary from $\approx$50 ps until the end of the investigated time interval (1 ns). By analogy with the spectra[23] of long-lived photointermediates of $[Re(Cl)(CO)_3(stpy)_2]$ and $[Re(stpy)(CO)_3(bpy)]^+$, this monotonic absorption is tentatively attributed to an ^3IL_p(MeDpe$^+$) state, in which the MeDpe$^+$ ligand is twisted by about 90° around the C=C bond (the subscript "p" denotes an approximately perpendicular orientation of the pyridine and pyridinium rings). This assignment is supported by time-resolved infrared (TRIR) spectra (see below). The ^3IL_p(MeDpe$^+$) state is the key isomerization intermediate, as in the case of the stpy complexes.[23] Its observation fully agrees with the photoisomerization of $[Re(MeDpe^+)(CO)_3(bpy)]^{2+}$ under stationary photolysis. The decay kinetics were measured at 500 nm and the two lifetimes estimated as 0.4–0.6 ps (90%) and 7–11 ps (10%) were attributed to the population decay of the ^{3}MLCT(MeDpe$^+$) and ^{3}MLCT(bpy) states, respectively. The much faster decay kinetics of the ^{3}MLCT excited states in $[Re(MeDpe^+)(CO)_3(bpy)]^{2+}$ relative to $[Re(Cl)(CO)_3(MeDpe^+)_2]^{2+}$ seems to be caused by the presence of a lower-lying excited state, presumably ^{3}IL(MeDpe$^+$), which is rapidly populated from the MLCT states.

Time-resolved resonance Raman spectroscopy: Time-resolved resonance Raman (TR^3) spectra of both complexes (Figure 5c,d) were measured after excitation at 400 nm and probed at wavelengths close to the short wavelength maximum of the excited state absorption spectrum, 510 and 525 nm for $[Re(Cl)(CO)_3(MeDpe^+)_2]^{2+}$ and $[Re(MeDpe^+)(CO)_3(bpy)]^{2+}$, respectively. The excited state of $[Re(Cl)(CO)_3(MeDpe^+)_2]^{2+}$ gives a very strong resonance Raman signal with bands at 1630 (sh), 1560 (s), 1473 (sh), 1332 (m), 1253 (s), 1168 (sh), 1009 (m), and 876 cm^{-1} (m) (peak positions measured at 50 ps). The bands can be correlated with their ground state counterparts (Figure 5), although the complexity of the molecules makes the assignment difficult. The strongest ν(C=C)/δ(CH) Raman band at 1634 cm^{-1} shifts upon excitation downwards by -76 cm^{-1}, indicating weakening of the C=C bond in the ^{3}MLCT(MeDpe$^+$) state. At early times, the peak maxima undergo a dynamic shift by about $+5$ cm^{-1} with lifetimes between 10–20 ps, due to vibrational cooling.[56,59,60] The band areas decay with kinetics commensurate with those of the TA bands.

The TR^3 spectrum of $[Re(MeDpe^+)(CO)_3(bpy)]^{2+}$ measured immediately after 400 nm excitation (Figure 5d) shows two prominent bands at about 1581 and 1255 cm^{-1}, which are attributed to the MeDpe$^\bullet$ ligand in the ^{3}MLCT(MeDpe$^+$) state by analogy with the TR^3 spectrum of $[Re(Cl)(CO)_3(MeDpe^+)_2]^{2+}$. However, the TR^3 signal of $[Re(MeDpe^+)(CO)_3(bpy)]^{2+}$ is much weaker and decays faster than that of $[Re(Cl)(CO)_3(MeDpe^+)_2]^{2+}$. Both bands disappear by 4 ps and no further Raman features are seen. The short lifetime agrees with the initial fast ($\approx$0.6 ps) decay component of the $\approx$500 nm TA band. The absence of Raman bands belonging to the ^{3}MLCT(bpy) state is understandable in view of their previously noticed weakness in picosecond TR^3 spectra of Re–tricarbonyl–bipyridine complexes.[34,56]

Time-resolved infrared spectroscopy: More detailed structural information on the excited states and photointermedi-

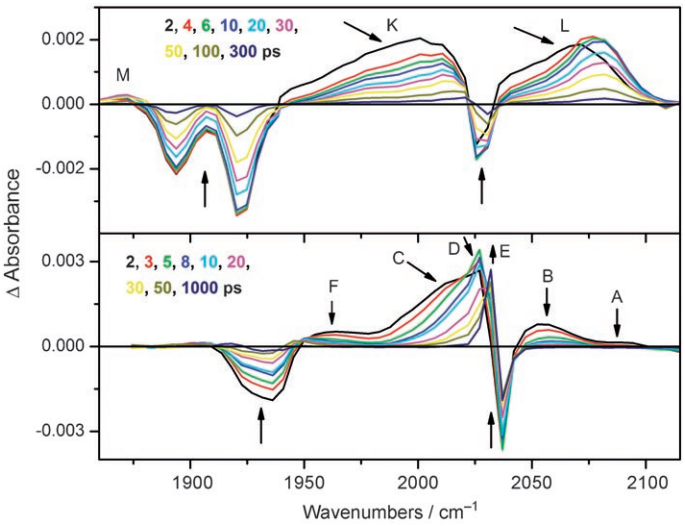

Figure 7. Difference time-resolved infrared spectra of $[Re(Cl)(CO)_3(MeDpe^+)_2]^{2+}$ in MeCN (top) and $[Re(MeDpe^+)(CO)_3(bpy)]^{2+}$ in CH_2Cl_2 (bottom) measured after 400 nm, ≈150 fs excitation. Experimental points are separated by about 5 cm^{-1}. (Spectra in complementary solvents: $[Re(Cl)(CO)_3(MeDpe^+)_2]^{2+}$ in CH_2Cl_2 and $[Re(MeDpe^+)(CO)_3(bpy)]^{2+}$ in MeCN are shown in the Supporting Information, Figures S1 and S2, respectively.).

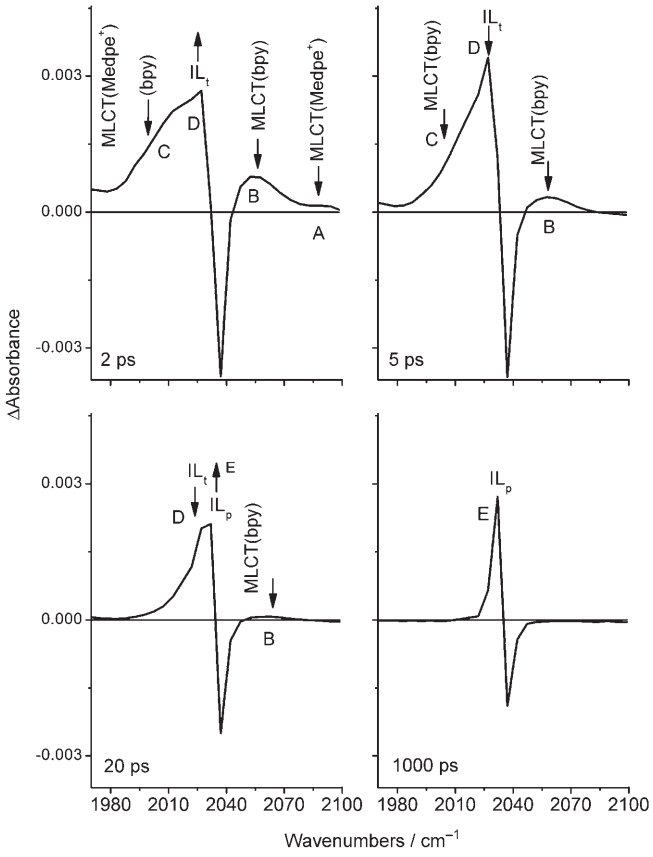

Figure 8. Difference time-resolved infrared spectra of $[Re(MeDpe^+)(CO)_3(bpy)]^{2+}$ in CH_2Cl_2, showing the A′(1) ν(CO) modes, measured at 2, 5, 20, and 1000 ps after excitation at 400 nm. The peaks are described using the labels from Figure 7 and assigned to individual states.

ates is provided by TRIR spectra in the region of the ν(CO) vibrations of the $Re(CO)_3$ moiety (Figures 7 and 8). The positive and negative spectral features correspond to the photogenerated transient and the depleted ground state population (bleach), respectively. Following excitation of $[Re(Cl)(CO)_3(MeDpe^+)_2]^{2+}$ in MeCN at 400 nm, the bleach ground state bands appear at 1893, 1923, and 2028 cm^{-1} and are attributed[50] to the A′(2), A″, and A′(1) ν(CO) modes, respectively. The A′(1) ν(CO) bleach intensity is smaller than expected from the ground state FTIR spectrum because of a strong overlap with a positive transient IR absorption. Two broad excited state bands appear at ≈2010 cm^{-1} with a shoulder at 1980 cm^{-1} (denoted K in Figure 7) and 2080 cm^{-1} (L) which are attributed to A′(2)+A″ and A′(1) ν(CO) excited state vibrations, respectively. (Peak wavenumbers were measured at time delays ≥20 ps.) In addition, a weak feature is seen at about 1870 cm^{-1} (M), which is indicative of a very small population of a ^{3}IL-$(MeDpe^+)$ state. The spectrum measured in CH_2Cl_2 shows identical behavior, the excited state bands occur at 1970, 2004, and 2070 cm^{-1} (Figure S1). The large upward shift of the bands K and L from their respective ground state positions shows[2,50,56,61–66] that they belong to the ^{3}MLCT-$(MeDpe^+)$ excited state(s). Characteristic for a ^{3}MLCT state, the A′(1) band shift is larger in MeCN than in CH_2Cl_2, 52 and 45 cm^{-1}, respectively. It is also larger than was observed[50] for an analogous complex $[Re(Cl)(CO)_3(4,4'\text{-bipyridine})_2]$: +30 cm^{-1} in CH_2Cl_2. This shows that the electron depopulation of the $Re(CO)_3$ moiety upon MLCT excitation is greater for $[Re(Cl)(CO)_3(MeDpe^+)_2]^{2+}$, supporting the conclusion that the excited electron is predominantly located on the distant −CH=CH−Py^+Me unit, which is largely electronically decoupled from the Re center. The TRIR spectra also show that the initially formed ^{3}MLCT$(MeDpe^+)$ state undergoes vibrational cooling between 2 and 20 ps, which is manifested by a ≈10 cm^{-1} dynamic shift to higher wavenumbers and small (≈3 cm^{-1}) narrowing. Although no detailed TRIR kinetic study was performed, the decay kinetics at 2081 cm^{-1} occur with a principal lifetime of 40–47 ps, and an unresolved slow component (200–500 ps), in a qualitative agreement with the TA. The decay of the TRIR signal is completed within 1 ns.

TRIR spectra of $[Re(MeDpe^+)(CO)_3(bpy)]^{2+}$ in CH_2Cl_2 show bleached ground state bands at 1929 cm^{-1} (A′(2)+A″) and 2035 cm^{-1} (A′(1)), see Figures 7 and 8. Relative intensities of the bleaches do not correspond to the FTIR spectrum, indicating the presence of overlapping excited state bands. At 2 ps, a broad transient band is seen at 2055 cm^{-1} (labeled B) and is blue-shifted from the A′(1) ν(CO) bleach by about +30 cm^{-1}. This feature is characteristic[2,56,62–66] of a MLCT(bpy) state. It occurs at similar energies in analogous complexes[23,34] such as $[Re(stpy)(CO)_3(bpy)]^+$ or $[Re(MQ^+)(CO)_3(dmb)]^{2+}$. Another weak transient associated with the A′(1) ν(CO) bleach is found at 2085 cm^{-1} (A). Its large upward shift is comparable with that found for ^{3}MLCT$(MeDpe^+)$ in $[Re(Cl)(CO)_3(MeDpe^+)_2]^{2+}$ or ^{3}MLCT-(MQ^+)[34] in $[Re(MQ^+)(CO)_3(bpy)]^{2+}$. Hence, the transient

A is assigned to the ^{3}MLCT(MeDpe$^+$) excited state. Its weak intensity results from the excited state having a very short lifetime of $\approx$0.6 ps, which means that most of the ^{3}MLCT(MeDpe$^+$) population have decayed by the time the first TRIR spectrum was measured. At lower wavenumbers, a broad feature occurs between 1980 and 2030 cm^{-1}. It is composed of several bands due to A′(2) vibrations[63,64] of ^{3}MLCT states (C) and A′(1) vibrations of IL states (D, E). Another band due to A″ vibration[63,64] of the ^{3}MLCT states is seen at about 1965 cm^{-1} (F). A very similar behavior was observed in MeCN (see Figure S2). As expected, the A′(1) bands of ^{3}MLCT(MeDpe$^+$) and ^{3}MLCT(bpy) occur at higher wavenumbers than in CH_2Cl_2, at $\approx$2105 and 2072 cm^{-1}, respectively.

The temporal evolution of the TRIR spectra of [Re(MeDpe$^+$)(CO)$_3$(bpy)]$^{2+}$ is shown in Figure 7, while Figure 8 shows detailed snapshots of the high-energy region. Between 2 and 4 ps, the features due to ^{3}MLCT(MeDpe$^+$) vanish, shown by the disappearance of the band A at 2085 cm^{-1}, fast narrowing in the region C, and rapidly decreasing intensity of F. This behavior agrees with the fast initial excited state decay observed by TA and TR^3. The ^{3}MLCT(bpy) band B (2055 cm^{-1}) and the residual absorptions F and C decay with a lifetime of 5–10 ps.[67] The band D at 2027 cm^{-1} increases in intensity by about 30% concomitantly with the decay of the ^{3}MLCT spectral features, reaching its maximum height by 5 ps. By analogy with [Re(stpy)(CO)$_3$(bpy)]$^+$, we attribute[23] this band to a MeDpe$^+$ localized ππ* intraligand state ^{3}IL$_t$, in which the *trans* (t) configuration of the pyridine and pyridinium rings is preserved. After $\approx$5 ps, the ^{3}IL$_t$ band at 2027 cm^{-1} (D) starts to decay, while another sharp band E grows in at 2032 cm^{-1}. This is exactly the behavior that we have described[23] for the photoisomerizing complex [Re(stpy)(CO)$_3$(bpy)]$^+$. This analogy allows us to attribute the band E to the ^{3}IL$_p$ state, in which the pyridine and pyridinium units of MeDpe$^+$ are twisted perpendicularly around the C=C bond. (Hence, the subscript "p" in ^{3}IL$_p$.) The presence of an isosbestic point at $\approx$2030 cm^{-1} indicates that the ^{3}IL$_t$→^{3}IL$_p$ conversion occurs as a clean, direct process. Its time constant was estimated as 21.3±0.6 ps from the decay of the band D. Once formed, the ^{3}IL$_p$ band E stays static until the end of the time interval investigated, 1 ns. Additional evidence for the population of the ^{3}IL$_t$ and ^{3}IL$_p$ states is provided by the broad low-frequency absorption which extends from about 1950 to 1895 cm^{-1}. The growth of this band is responsible for the apparent decrease of the overlapping broad bleach band at $\approx$1935 cm^{-1}, Figure 7. A very similar time evolution was observed in MeCN (see Figure S2). The ^{3}MLCT(bpy) lifetime is a little longer in MeCN than in CH_2Cl_2, 12–18 ps. The rate of the ^{3}IL$_t$→^{3}IL$_p$ conversion cannot be determined because of a large overlap of the corresponding IR bands.

Discussion

The experimental observations essential to understanding the complex excited state behaviors of [Re(Cl)(CO)$_3$(MeDpe$^+$)$_2$]$^{2+}$ and [Re(MeDpe$^+$)(CO)$_3$(bpy)]$^{2+}$ can be summarized as follows:

1) The first reduction step of [Re(Cl)(CO)$_3$(MeDpe$^+$)$_2$]$^{2+}$ and [Re(MeDpe$^+$)(CO)$_3$(bpy)]$^{2+}$ is localized on the MeDpe$^+$ ligand, which is easily reducible at about −1.1 V versus Fc/Fc$^+$. The bpy localized reduction in [Re(MeDpe$^+$)(CO)$_3$(bpy)]$^{2+}$ is about 0.4 V more negative.
2) The free MeDpe$^+$ ligand and [Re(MeDpe$^+$)(CO)$_3$(bpy)]$^{2+}$ undergo efficient *trans*→*cis* isomerization under stationary near-UV irradiation, while [Re(Cl)(CO)$_3$(MeDpe$^+$)$_2$]$^{2+}$ is photostable.
3) Irradiation at 400 nm, used in the time-resolved spectroscopic experiments, excites both [Re(Cl)(CO)$_3$(MeDpe$^+$)$_2$]$^{2+}$ and [Re(MeDpe$^+$)(CO)$_3$(bpy)]$^{2+}$ predominantly into the ^{1}MLCT(MeDpe$^+$) state. Since intersystem crossing (ISC) in these type of complexes occurs on a femtosecond timescale,[3,23] all the picosecond dynamics described herein can be attributed to the triplet excited-state manifold.
4) Picosecond visible TA, TRIR, and TR^3 measurements identify the lowest excited state of [Re(Cl)(CO)$_3$(MeDpe$^+$)$_2$]$^{2+}$ as ^{3}MLCT(MeDpe$^+$), which can be formally viewed as [Re^{II}(Cl)(CO)$_3$(MeDpe$^{\bullet}$)(MeDpe$^+$)]$^{2+}$. It decays directly to the ground state with lifetimes of $\approx$40 ps (principal) and a 430 ps (minor). The photobehavior of [Re(Cl)(CO)$_3$(MeDpe$^+$)$_2$]$^{2+}$ is shown in Scheme 1.

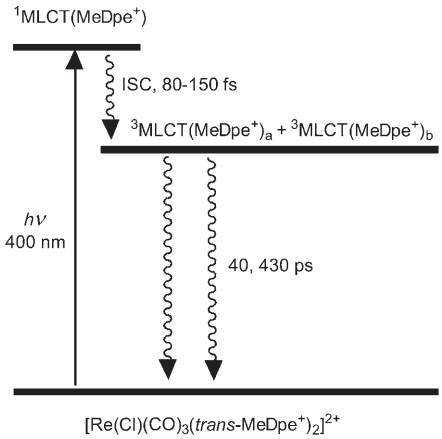

Scheme 1. Proposed mechanism of excited state deactivation in [Re(Cl)(CO)$_3$(MeDpe$^+$)$_2$]$^{2+}$. The subscripts a and b denote the two ^{3}MLCT states of a similar origin or conformations, the population of which is indicated by the biexponential decay kinetics. ISC lifetime estimate is based on data from ref.[3]

5) Irradiation of [Re(MeDpe$^+$)(CO)$_3$(bpy)]$^{2+}$ leads initially to simultaneous population of two close lying excited

states ^{3}MLCT(MeDpe$^+$) and ^{3}MLCT(bpy), which decay with lifetimes of $\approx$0.6 and $\approx$10 ps, respectively, into a ^3IL_t state, Scheme 2. ^3IL_t is a MeDpe$^+$ localized $^3\pi\pi^*$ excited state, in which the *trans* configuration of the pyridine and pyridinium rings is preserved. The ^{3}MLCT$\rightarrow$ ^3IL_t conversion is clearly manifested by the change of the ν(CO) TRIR spectral pattern, whereby decay of the broad, up-shifted A′(1) band is accompanied by increase of a narrow, down-shifted band, Figures 7 and 8.

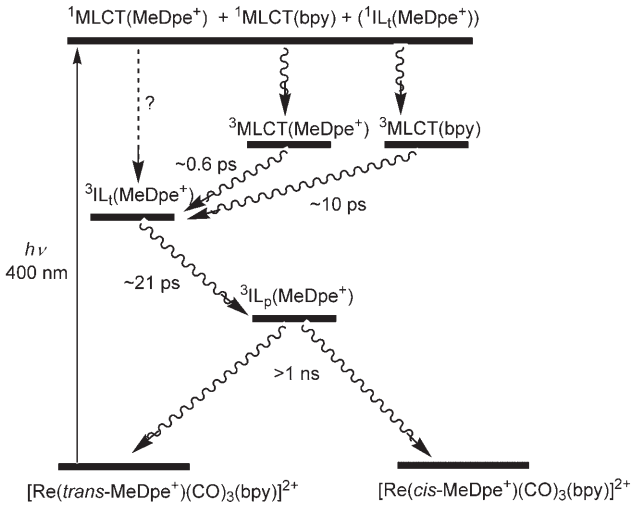

Scheme 2. Proposed mechanism of excited state deactivation in [Re(MeDpe$^+$)(CO)$_3$(bpy)]$^{2+}$.

6) The ^3IL_t state undergoes conversion after $\approx$21 ps to another ^{3}IL state, in which the ν(CO) A′(1) band lies only 4–5 cm^{-1} higher in energy. By analogy[23] with [Re(stpy)(CO)$_3$(bpy)]$^+$ and [Re(Cl)(CO)$_3$(stpy)$_2$], this process is attributed to a half-rotation of the MeDpe$^+$ ligand around the central C=C bond by about 90°. The pyridine and pyridinium rings are approximately perpendicular in the final state, which is denoted ^3IL_p. This state is the key intermediate of the *trans*$\rightarrow$*cis* isomerization, which follows on a much slower, presumably nanosecond, timescale. Excited state behavior of [Re(MeDpe$^+$)(CO)$_3$(bpy)]$^{2+}$ is shown in Scheme 2.
7) Excited state behavior of either complex is essentially identical in MeCN and CH_2Cl_2.

The striking difference in the excited state behavior and photochemistry of [Re(Cl)(CO)$_3$(MeDpe$^+$)$_2$]$^{2+}$ and [Re(MeDpe$^+$)(CO)$_3$(bpy)]$^{2+}$ is caused by the different order of ^{3}MLCT and ^3IL_t excited states, which themselves have different reactivity. The ^{3}MLCT(MeDpe$^+$) state is unreactive, and nonradiative decay to the ground state by back electron transfer MeDpe$^{\bullet}\rightarrow$Re^{II} is its only deactivation pathway. The lack of isomerization in ^{3}MLCT(MeDpe$^+$) as well as in the reduction products [Re(Cl)(CO)$_3$(MeDpe$^{\bullet}$)$_2$] and [Re(MeDpe$^{\bullet}$)(CO)$_3$(bpy)]$^+$, free Me$_2$dpe$^{+\bullet}$[44] or in a I$^-\rightarrow$Me$_2$dpe^{2+} CT excited state of an ion pair [Me$_2$dpe^{2+}]$\cdot$2I$^-$[54,55] shows that one-electron reduction of the MeDpe$^+$ ligand is not sufficient to activate the −CH=CH− unit toward isomerization. The photochemical stability of [Re(Cl)(CO)$_3$(MeDpe$^+$)$_2$]$^{2+}$ is the direct consequence of ^{3}MLCT(MeDpe$^+$) being the lowest excited state.

The situation is different for [Re(MeDpe$^+$)(CO)$_3$(bpy)]$^{2+}$. Although optical excitation initially leads to population of ^{3}MLCT states, they are not the lowest excited states. The ^3IL_t state lies lower in energy and is populated by ultrafast conversion from ^{3}MLCT(MeDpe$^+$) and ^{3}MLCT(bpy), whose lifetimes are thus shortened by several orders of magnitude, to 0.6 and $\approx$10 ps for, respectively. (A typical lifetime of a ^{3}MLCT(bpy) decay to the ground state would be $\approx$230 ns.[68]) Internal conversion from either ^{3}MLCT state to ^3IL_t(MeDpe$^+$) occurs over a small energy gap. The ^{3}MLCT(MeDpe$^+$)$\rightarrow$$^3IL_t$(MeDpe$^+$) conversion amounts to an electron transfer from a lower-lying doubly-occupied π(MeDpe$^{\bullet}$) orbital to the singly-occupied dπ(Re) orbital in ^{3}MLCT(MeDpe$^+$). On the other hand, ^{3}MLCT(bpy)$\rightarrow$$^3IL_t$(MeDpe$^+$) requires a double electron exchange and can be viewed as a Dexter-type intramolecular energy transfer from the {Re(CO)$_3$(bpy)} chromophore to the MeDpe$^+$ ligand. It is only a little slower than the analogous ^{3}MLCT(bpy)$\rightarrow$$^3IL_t$(stpy) conversion in [Re(stpy)(CO)$_3$(bpy)]$^+$, 3.5 ps.[23] Depopulation of the π(C=C) orbital and partial population of the π^* orbital in ^3IL_t loosen the C=C bond, allowing for rotation into a geometry, in which the pyridine and pyridinium rings are approximately perpendicular, ^3IL_p(MeDpe$^+$). This partial rotation is a common step in the photoisomerization of −CH=CH− or −N=N− bonds from triplet intraligand excited states. In addition to [Re(MeDpe$^+$)(CO)$_3$(bpy)]$^{2+}$, this was observed for the $^3\pi\pi^*$ state of stpy in [Re(Cl)(CO)$_3$(stpy)$_2$] and [Re(stpy)(CO)$_3$(bpy)]$^+$[23] and the $^3n\pi^*$ state of *trans*-4-phenyl-azopyridine (papy) in [Re(Cl)(CO)$_3$(papy)$_2$] and [Re(papy)(CO)$_3$(bpy)]$^+$.[24] Its rate is almost two times slower for MeDpe$^+$ ($\approx$21 ps) than stpy (11–12 ps),[23] presumably because of a larger delocalization of the π^* electron in MeDpe$^+$, resulting in a higher barrier. The fate of ^3IL_p(MeDpe$^+$) on a nanosecond timescale was not studied. We assume that ^3IL_p(MeDpe$^+$) undergoes ISC to the twisted ground state, followed either by further rotation around the central −CH−CH− bond forward to the *cis* isomer or backwards to the original *trans* geometry, similar to [Re(Cl)(CO)$_3$(stpy)$_2$], [Re(stpy)(CO)$_3$(bpy)]$^+$, and [Re(1,2-dipyridylethylene)(CO)$_3$(bpy)]$^+$, in which this process occurs with a lifetime of about 17 ns.[40,69] Stationary photolysis of [Re(MeDpe$^+$)(CO)$_3$(bpy)]$^{2+}$ indicates that isomerization prevails, and the corresponding quantum yield is rather high. It needs to be emphasized that the long-lived twisted intermediate ^3IL_p is involved only in isomerization from a triplet state, sensitized by coordination to a heavy metal. Free stilbene, stpy, papy, or azobenzene isomerize from their singlet states through a conical intersection with the ground state, which occurs with picosecond lifetimes, without observable twisted intermediates.[23,24,70–73]

The difference in the excited state dynamics and photoreactivity of $[Re(Cl)(CO)_3(MeDpe^+)_2]^{2+}$ and $[Re(MeDpe^+)(CO)_3(bpy)]^{2+}$ demonstrates how subtle structural differences control excited state behavior. The $\{Re(Cl)(CO)_3\}$ moiety in $[Re(Cl)(CO)_3(MeDpe^+)_2]^{2+}$ is an electron donor due to the presence of the Cl ligand, pushing the unreactive ^{3}MLCT(MeDpe$^+$) below the ^3IL_t. Decay to the ground state is then the only possible deactivation pathway. The energy balance is different in $[Re(MeDpe^+)(CO)_3(bpy)]^{2+}$, in which the two electron acceptor ligands (i.e., bpy and MeDpe$^+$) pull the MLCT states to higher energies, above the reactive ^3IL_t state. Another interesting comparison can be made between MeDpe$^+$ and stpy complexes. Replacement of a phenyl ring in stpy with the strong electron-acceptor methylpyridinium in MeDpe$^+$ introduces MLCT(MeDpe$^+$) states into its Re complexes. Lying below the ^{3}IL states in the case of $Re(MeDpe^+)_2$, the ^{3}MLCT(MeDpe$^+$) state prevents photoisomerization, whereas $[Re(Cl)(CO)_3(stpy)_2]$ is photoreactive. On the other hand, the excited state behavior and photochemistry of $[Re(MeDpe^+)(CO)_3(bpy)]^{2+}$ and $[Re(stpy)(CO)_3(bpy)]^+$ are very similar, since ^3IL_t is the lowest excited state in both complexes. The last comparison to be discussed is between $[Re(MeDpe^+)(CO)_3(bpy)]^{2+}$ and $[Re(MQ^+)(CO)_3(4,4'\text{-di-Me-bpy})]^{2+}$. The latter complex shows an ultrafast (8.3 ps in MeCN) interligand electron transfer (ILET) $bpy^{\bullet-}\rightarrow MQ^+$ from its ^{3}MLCT(bpy) state.[34,35] There is no evidence for an analogous $bpy^{\bullet-}\rightarrow$ MeDpe$^+$ ILET in excited $[Re(MeDpe^+)(CO)_3(bpy)]^{2+}$, although it could occur with a comparable driving force, $\approx$0.4 eV. However, the longer distance (through-bond and/or through-space) between $bpy^{\bullet-}$ and the pyridinium ring of MeDpe$^+$ will slow down the ILET in $[Re(MeDpe^+)(CO)_3(bpy)]^{2+}$ relative to $[Re(MQ^+)(CO)_3(bpy)]^{2+}$. The lack of ILET in $[Re(MeDpe^+)(CO)_3(bpy)]^{2+}$ could simply be another consequence of the presence of a low-lying ^3IL_t(MeDpe$^+$) state, which opens a faster deactivation channel ^{3}MLCT(bpy)$\rightarrow{}^3IL_t$(MeDpe$^+$), making ILET uncompetitive.

Conclusion

The multifunctional cationic ligand MeDpe$^+$ (*N*-methyl-4-[*trans*-2-(4-pyridyl)ethenyl]pyridinium) forms stable complexes with $Re^I(CO)_3$, into which it introduces low-lying MLCT and IL ($\pi\pi^*$) excited states. Reduction to a coordinated MeDpe$^\bullet$ radical can be accomplished either electrochemically or, transiently, by MLCT electronic excitation. Reduction does not activate the ligand toward *trans*$\rightarrow$*cis* isomerization. The Re$\rightarrow$MeDpe$^+$ ^{3}MLCT excited state is short-lived (tens-to-hundreds ps), non-emissive, and unreactive. In the absence of any lower-lying excited states, ^{3}MLCT(MeDpe$^+$) decays nonradiatively to the ground state by a $\pi^*\rightarrow d\pi$(Re) back electron transfer. This is the case in the photostable complex $[Re(Cl)(CO)_3(MeDpe^+)_2]^{2+}$. Population of an ^{3}IL excited state results in efficient *trans*$\rightarrow$*cis* isomerization, which involves a $\approx$21 ps half-rotation around the C=C bond to form a nanosecond-lived intermediate with a perpendicular orientation of the aromatic rings. This is the case of the complex $[Re(MeDpe^+)(CO)_3(bpy)]^{2+}$, in which ^{3}IL is the lowest excited state. ^{3}IL is efficiently populated by internal conversion from ^{3}MLCT(MeDpe$^+$) and ^{3}MLCT(bpy) excited states by intramolecular electron and energy transfer, respectively. The ^{3}MLCT$\rightarrow{}^3$IL conversion is an example of ultrafast intramolecular sensitization of ligand-based triplet state photochemistry, a process that could find use in molecular devices. It is fast enough to prevail over potentially competing, thermodynamically favorable, interligand electron transfer from the ^{3}MLCT(bpy) state.

Excited state dynamics in Re^I complexes with the MeDpe$^+$ ligand are determined by the energetic balance between the low-lying ^{3}MLCT and ^{3}IL excited states, which can be fine-tuned by structural variations. $[Re(Cl)(CO)_3(MeDpe^+)_2]^{2+}$ and $[Re(MeDpe^+)(CO)_3(bpy)]^{2+}$ embody multifunctional complexes which combine rich photonic and redox behaviors and clearly show their structural control.

Experimental Section

Materials and preparations: Spectroscopic measurements were performed in acetonitrile (MeCN) or CH_2Cl_2, as purchased from Aldrich, spectrophotometric grade. Analytical grade tetrahydrofuran (THF), MeCN, and butyronitrile (PrCN) for electrochemical experiments (Acros Chimica), were dried by standard procedures[74] and freshly distilled prior to use. The supporting electrolyte Bu_4NPF_6 (Bu = *n*-butyl; Aldrich) was recrystallized twice from absolute ethanol and dried in vacuo at 80 °C for 3 days. Elemental analyses were conducted in H. Kolbe Mikroanalytisches Laboratorium, Mülheim an der Ruhr, Germany.

***trans*-*N*-(Methyl)-4,4′-dipyridiniumethylene hexafluorophosphate ([MeDpe]PF$_6$)**: A procedure based on methylating picoline with methyl iodide, followed by a coupling reaction with 4-pyridinecarboxaldehyde was used as described in the literature.[75] ^{1}H NMR ([D$_3$]acetonitrile, 270 MHz): δ = 4.24 (s, 3H; methyl CH_3), 7.58 (d, J = 16.6 Hz, 1H; ethylenic CH), 7.67 (d, J = 6.0 Hz, 2H; aromatic CH), 7.73(d, J=16.6 Hz, 1H; ethylenic CH), 8.07 (d, J = 6.9 Hz, 2H; aromatic CH), 8.53 (d, J = 6.6 Hz, 2H; aromatic CH), 8.67 ppm (d, J = 6.4 Hz, 2H; aromatic CH)

[Re(Cl)(CO)$_3$(MeDpe)$_2$][PF$_6$]$_2$: [Re(Cl)(CO)$_5$] (204 mg, 0.56 mmol) and [MeDpe]PF$_6$, (342 mg, 1.70 mmol) were heated at reflux in dry methanol (50 mL) for 3.5 h. The reactants were initially insoluble, but produced a clear solution after 20 min of reflux, followed by formation of a yellow precipitate. The yellow solid was collected by filtering the hot suspension and washed with hot methanol (2 mL). The product was repeatedly recrystallized from dry methanol until pure. Yield 87%; FTIR (acetonitrile): $\tilde{\nu}$ = 2025 (s), 1921 (s), 1893 cm^{-1} (s); ^{1}H NMR ([D$_6$]acetone, 270 MHz): δ = 4.57 (s, 6H; CH_3), 7.84 (d, J = 6.9 Hz, 4H; aromatic CH), 7.93 (d, J = 16.3 Hz, 2H; ethylenic CH), 8.05 (d, J = 16.6 Hz, 2H; ethylenic CH), 8.41 (4H; d, J = 6.4 Hz, aromatic CH), 8.89 (4H; d, J = 6.5 Hz, aromatic CH), 9.02 ppm (4H; d, J = 6.3 Hz, aromatic CH); ^{13}C NMR ([D$_6$]acetone, 67.9 MHz): δ = 47.60, 123.97, 125.27, 130.24, 136.33, 145.38, 145.92, 151.92, 154.36 ppm; ES-MS: m/z: 845.3 [M^+−PF$_6$]; elemental analysis calcd (%) for $C_{26}H_{21}F_{12}N_4O_3P_2Re$ (990.1): C 35.18, H 2.65, N 5.66; found: C 34.92, H 2.72, N 5.60.

[Re(CO)$_3$(bpy)(MeDpe)][PF$_6$]$_2$: [Re(OTf)(CO)$_3$(bpy)][68] (1.185 g, 2.06 mmol; OTf = trifluoromethanesulfonate) and [MeDpe]PF$_6$ (1.057 g, 3.09 mmol) were heated at reflux in dry methanol (100 mL) for 12 h. The hot reaction mixture was filtered and NH_4PF_6 (1 g) was added to the filtrate. The precipitate was collected by filtration and purified by repeated recrystallization from methanol. Yield 68%; FTIR (CH_2Cl_2): $\tilde{\nu}$ = 2036 (s), 1933 cm^{-1} (br); ^{1}H NMR ([D$_6$]acetone, 270 MHz): δ = 4.52 (s, 3H; CH_3),

7.71 (d, $J=6.6$ Hz, 2H; aromatic CH), 7.78 (d, $J=16.7$ Hz, 1H; ethylenic CH), 7.89(d, $J=16.7$ Hz, 1H; ethylenic CH), 8.00 (dd, $J=7.2$ Hz, 2H; aromatic CH), 8.30 (d, $J=6.9$ Hz, 2H; aromatic CH), 8.45 dd, $J=7.7$ Hz, (2H; aromatic CH), 8.61 (d, $J=6.7$ Hz, 2H; aromatic CH), 8.72 (d, $J=8.5$ Hz, 2H; aromatic CH), 8.98 (d, $J=7.1$ Hz, 2H; aromatic CH), 9.48 ppm (d, $J=4.8$ Hz, 2H; aromatic CH); ^{13}C NMR ([D$_6$]acetone, 67.9 MHz): $\delta=47.77$ (CH_3), 124.73, 124.98, 125.21, 129.24, 130.80, 135.57, 141.56, 145.90, 146.09, 151.60, 152.85, 154.24, 156.06, 191.50 (CO), 195.51 ppm (CO); ES-MS: m/z: 769.2 [M^+-PF_6]; elemental analysis calcd (%) for $C_{26}H_{21}F_{12}N_4O_3P_2Re$ (913.6): C 34.18, H 2.32, N 6.13; found: C 33.98, H 2.27, N 6.11.

Instrumentation: Ground state resonance Raman spectra were obtained on an instrument described previously,[23] by using a Coherent Innova 90–5 UV argon-ion laser with a power output of about 50 mW at 457.9 nm.

Time-resolved UV/Vis absorption spectra (TA) were measured by using the experimental setup at the Van't Hoff Institute for Molecular Sciences, University of Amsterdam.[76] A ≈130 fs, 390 nm pump pulse was generated by frequency doubling of the titanium sapphire laser output. White light continuum probe pulses were generated by focusing the 780 nm fundamental in a sapphire plate.

Time-resolved IR (TRIR) and Kerr-gate resonance Raman (TR^3) experiments used the equipment and procedures described in detail previously.[34,66,77–81] In short, the sample solution was excited (pumped) at 400 nm, using frequency-doubled pulses from a titanium sapphire laser of ≈150 fs duration (full width at half maximum, FWHM) TRIR, and pulses of 1–2 ps duration were used for the Raman studies. TRIR spectra were probed with IR (≈150 fs) pulses obtained by difference frequency generation. The IR probe pulses cover a spectral range about 200 cm^{-1} wide and are tunable from 1000 to 5000 cm^{-1} (i.e., 2–10 μm). Kerr-gate TR^3 spectra were probed at 475 nm using one-photon absorption (OPA). A Kerr-gate was employed to remove all long-lived emission from the Raman signal. TR^3 spectra were corrected for the Raman signal due to the solvent and the solute ground state by subtracting the spectra obtained at negative time delays (−50, −20 ps) and by subtracting any weak residual fluorescence emission that passed through the Kerr-gate. The sample solutions for picosecond TR^3 and TRIR experiments flowed as a 0.5 mm open jet and through a 0.5 mm CaF_2 raster-scanned cell, respectively. All spectral fitting procedures were performed using Microcal Origin 7 software.

Cyclic voltammograms were recorded with EG&G PAR Model 283 potentiostat using an air-tight single-compartment three-electrode cell placed in a Faraday cage. The cell contained a platinum disk working electrode (apparent surface area of 0.42 mm^2, polished carefully with a 0.25 μm diamond paste, Oberflächentechnologien Ziesmer, Kempen, Germany), a platinum wire auxiliary electrode, and a silver wire pseudoreference electrode. The standard[82] ferrocene/ferrocenium (Fc/Fc^+) redox couple served as an internal reference system. Cooling of the cell was achieved with slurry of dry ice in acetone (208 K).

IR and UV/Vis spectral changes at various temperatures were monitored spectroelectrochemically using optically transparent thin-layer electrochemical (OTTLE) cells[83–85] equipped with Pt minigrid working electrodes and CaF_2 windows. Thin-layer cyclic voltammograms were recorded in the course of each spectroelectrochemical run for a precise potential control and monitoring the progress of electrolysis by the decrease of the Faradaic current. The spectroelectrochemical samples typically contained 10^{-3} M (UV/Vis) or 3×10^{-3} M (IR) rhenium complex and 3×10^{-1} M Bu_4NPF_6 supporting electrolyte. The potential of the minigrid working electrode was controlled by a PA4 (EKOM, Polná, Czech Republic) potentiostat. IR spectra of the electrolyzed solutions were recorded with a Bruker Vertex 70 spectrometer (16 scans, resolution of 1 cm^{-1}, a DTGS detector). For low-temperature spectroelectrochemistry, the Bruker spectrometer was coupled to a sample compartment and a liquid N_2 cooled MCT (mercury–cadmium–telluride) detector taken from a Bio-Rad FTS 60. UV/Vis spectroelectrochemistry was conducted with a Hewlett Packard 8453 diode-array spectrophotometer.

Stationary photolysis was carried out using a LOT Oriel high-pressure Hg lamp with the appropriate filters. Irradiated solutions in aerated MeCN (absorbance between 0.5–1) were placed in 1 cm quartz cells and stirred during irradiation.

Acknowledgements

The financial support from EPSRC, STFC Rutherford Appleton Laboratory (CMSD43), and the European collaboration programme COST D14 is gratefully acknowledged. M. Groeneveld and T. Mahabiersing (both University of Amsterdam) are thanked for assistance at the ps TA and spectroelectrochemical measurements, respectively.

[1] D. J. Stufkens, A. Vlček Jr. , *Coord. Chem. Rev.* **1998**, *177*, 127.
[2] A. Vlček, Jr., S. Záliš, *Coord. Chem. Rev.* **2007**, *251*, 258.
[3] A. Cannizzo, A. M. Blanco-Rodríguez, A. Nahhas, J. Šebera, S. Záliš, A. Vlček, Jr., M. Chergui, *J. Am. Chem. Soc.* **2008**, *130*, in press.
[4] A. M. Blanco-Rodríguez, K. L. Ronayne, S. Záliš, J. Sýkora, M. Hof, A. Vlček, Jr., *J. Phys. Chem. A* **2008**, *112*, 3506.
[5] A. M. Blanco-Rodríguez, A. Gabrielsson, M. Motevalli, P. Matousek, M. Towrie, J. Šebera, S. Záliš, A. Vlček, Jr., *J. Phys. Chem. A* **2005**, *109*, 5016.
[6] G. J. Stor, D. J. Stufkens, A. Oskam, *Inorg. Chem.* **1992**, *31*, 1318.
[7] B. D. Rossenaar, D. J. Stufkens, A. Vlček, Jr., *Inorg. Chem.* **1996**, *35*, 2902.
[8] W. B. Connick, A. J. Di Bilio, M. G. Hill, J. R. Winkler, H. B. Gray, *Inorg. Chim. Acta* **1995**, *240*, 169.
[9] J. B. Asbury, E. Hao, Y. Wang, H. N. Ghosh, T. Lian, *J. Phys. Chem. B* **2001**, *105*, 4545.
[10] A. M. Blanco-Rodríguez, M. Busby, C. Grădinaru, B. R. Crane, A. J. Di Bilio, P. Matousek, M. Towrie, B. S. Leigh, J. H. Richards, A. Vlček, Jr., H. B. Gray, *J. Am. Chem. Soc.* **2006**, *128*, 4365.
[11] C.-C. Ko, W.-M. Kwok, V. W.-W. Yam, D. L. Phillips, *Chem. Eur. J.* **2006**, *12*, 5840.
[12] K. K.-W. Lo, K. H.-K. Tsang, K.-S. Sze, C.-K. Chung, T. K.-M. Lee, K. Y. Zhang, W.-K. Hui, C.-K. Li, J. S.-Y. Lau, D. C.-M. Ng, N. Zhu, *Coord. Chem. Rev.* **2007**, *251*, 2292.
[13] O. S. Wenger, L. M. Henling, M. W. Day, J. R. Winkler, H. B. Gray, *Inorg. Chem.* **2004**, *43*, 2043.
[14] C. A. Berg-Brennan, D. I. Yoon, R. V. Slone, A. P. Kazala, J. T. Hupp, *Inorg. Chem.* **1996**, *35*, 2032.
[15] J. D. Lewis, R. N. Perutz, J. N. Moore, *J. Phys. Chem. A* **2004**, *108*, 9037.
[16] S.-S. Sun, A. J. Lees, P. Y. Zavalij, *Inorg. Chem.* **2003**, *42*, 3445.
[17] A. Beyeler, P. Belser, L. De Cola, *Angew. Chem.* **1997**, *109*, 2878; *Angew. Chem. Int. Ed. Engl.* **1997**, *36*, 2779.
[18] J. D. Lewis, J. N. Moore, *Dalton Trans.* **2004**, 1376.
[19] H. D. Stoeffler, N. B. Thornton, S. L. Temkin, K. S. Schanze, *J. Am. Chem. Soc.* **1995**, *117*, 7119.
[20] V. W.-W. Yam, K. K.-W. Lo, K.-K. Cheung, R. Y.-C. Kong, *J. Chem. Soc. Dalton Trans.* **1997**, 2067.
[21] V. W.-W. Yam, K. K.-W. Lo, K.-K. Cheung, R. Y.-C. Kong, *J. Chem. Soc. Chem. Commun.* **1995**, 1191.
[22] J. Dyer, W. J. Blau, C. G. Coates, C. M. Creely, J. D. Gavey, M. W. George, D. C. Grills, S. Hudson, J. M. Kelly, P. Matousek, J. J. McGarvey, J. McMaster, A. W. Parker, M. Towrie, J. A. Weinstein, *Photochem. Photobiol. Sci.* **2003**, *2*, 542.
[23] M. Busby, P. Matousek, M. Towrie, A. Vlček, Jr., *J. Phys. Chem. A* **2005**, *109*, 3000.
[24] M. Busby, P. Matousek, M. Towrie, A. Vlček, Jr., *Inorg. Chim. Acta* **2007**, *360*, 885.
[25] I. P. Clark, M. W. George, F. P. A. Johnson, J. J. Turner, *Chem. Commun.* **1996**, 1587.
[26] S. Y. Reece, D. G. Nocera, *J. Am. Chem. Soc.* **2005**, *127*, 9448.
[27] P. Chen, T. D. Westmoreland, E. Danielson, K. S. Schanze, D. Anthon, P. E. Neveux, Jr., T. J. Meyer, *Inorg. Chem.* **1987**, *26*, 1116.

[28] P. Chen, R. Duesing, D. K. Graff, T. J. Meyer, *J. Phys. Chem.* **1991**, *95*, 5850.
[29] P. Chen, S. L. Mecklenburg, T. J. Meyer, *J. Phys. Chem.* **1993**, *97*, 13126.
[30] S. L. Mecklenburg, B. M. Peek, J. R. Schoonover, D. G. McCafferty, C. G. Wall, B. W. Erickson, T. J. Meyer, *J. Am. Chem. Soc.* **1993**, *115*, 5479.
[31] S. L. Mecklenburg, K. A. Opperman, P. Chen, T. J. Meyer, *J. Phys. Chem.* **1996**, *100*, 15145.
[32] A. M. Blanco-Rodríguez, A. Gabrielsson, M. Towrie, A. Vlček, Jr., unpublished results.
[33] D. J. Stufkens, *Comments Inorg. Chem.* **1992**, *13*, 359.
[34] D. J. Liard, M. Busby, I. R. Farrell, P. Matousek, M. Towrie, A. Vlček, Jr., *J. Phys. Chem. A* **2004**, *108*, 556.
[35] D. J. Liard, A. Vlček, Jr., *Inorg. Chem.* **2000**, *39*, 485.
[36] P. P. Zarnegar, C. R. Bock, D. G. Whitten, *J. Am. Chem. Soc.* **1973**, *95*, 4367.
[37] J. R. Shaw, R. T. Webb, R. H. Schmehl, *J. Am. Chem. Soc.* **1990**, *112*, 1117.
[38] M. K. Itokazu, A. S. Polo, N. Y. M. Iha, *J. Photochem. Photobiol. A* **2003**, *160*, 27.
[39] S.-S. Sun, A. J. Lees, *Organometallics* **2002**, *21*, 39.
[40] D. M. Dattelbaum, M. K. Itokazu, N. Y. M. Iha, T. J. Meyer, *J. Phys. Chem. A* **2003**, *107*, 4092.
[41] V. W.-W. Yam, V. C.-Y. Lau, L.-X. Wu, *J. Chem. Soc. Dalton Trans.* **1998**, 1461.
[42] J. D. Lewis, J. N. Moore, *Phys. Chem. Chem. Phys.* **2004**, *6*, 4595.
[43] S. Berger, A. Klein, W. Kaim, J. Fiedler, *Inorg. Chem.* **1998**, *37*, 5664.
[44] T. W. Ebbesen, R. Akaba, K. Tokumaru, M. Washio, S. Tagawa, Y. Tabata, *J. Am. Chem. Soc.* **1988**, *110*, 2147.
[45] P. S. Braterman, J.-I. Song, *J. Org. Chem.* **1991**, *56*, 4678.
[46] M. Krejčík, A. A. Vlček, *J. Electroanal. Chem. Interfacial Electrochem* **1991**, *313*, 243.
[47] F. Hartl, R. P. Groenestein, T. Mahabiersing, *Collect. Czech. Chem. Commun.* **2001**, *66*, 52.
[48] Y. F. Lee, J. R. Kirchhoff, R. M. Berger, D. Gosztola, *J. Chem. Soc. Dalton Trans.* **1995**, 3677.
[49] J. R. Schoonover, P. Chen, W. D. Bates, R. B. Dyer, T. J. Meyer, *Inorg. Chem.* **1994**, *33*, 793.
[50] D. R. Gamelin, M. W. George, P. Glyn, F.-W. Grevels, F. P. A. Johnson, W. Klotzbücher, S. L. Morrison, G. Russell, K. Schaffner, J. J. Turner, *Inorg. Chem.* **1994**, *33*, 3246.
[51] D. J. Stufkens, *Coord. Chem. Rev.* **1990**, *104*, 39.
[52] J. van Slageren, A. Klein, S. Záliš, D. J. Stufkens, *Coord. Chem. Rev.* **2001**, *219–221*, 937.
[53] R. W. Balk, D. J. Stufkens, A. Oskam, *J. Chem. Soc. Dalton Trans.* **1981**, 1124.
[54] T. W. Ebbesen, K. Tokumaru, M. Sumitani, K. Yoshihara, *J. Phys. Chem.* **1989**, *93*, 5453.
[55] T. W. Ebbesen, C. M. Previtali, T. Karatsu, T. Arai, K. Tokumaru, *Chem. Phys. Lett.* **1985**, *119*, 489.
[56] D. J. Liard, M. Busby, P. Matousek, M. Towrie, A. Vlček, Jr., *J. Phys. Chem. A* **2004**, *108*, 2363.
[57] B. D. Rossenaar, D. J. Stufkens, A. Vlček, Jr., *Inorg. Chim. Acta* **1996**, *247*, 247.
[58] K. Kalyanasundaram, *J. Chem. Soc. Faraday Trans. 2* **1986**, *82*, 2401.
[59] W. L. Weaver, L. A. Huston, K. Iwata, T. L. Gustafson, *J. Phys. Chem.* **1992**, *96*, 8956.
[60] K. Iwata, H. Hamaguchi, *J. Phys. Chem. A* **1997**, *101*, 632.
[61] P. Glyn, M. W. George, P. M. Hodges, J. J. Turner, *J. Chem. Soc. Chem. Commun.* **1989**, 1655.
[62] M. W. George, F. P. A. Johnson, J. R. Westwell, P. M. Hodges, J. J. Turner, *J. Chem. Soc. Dalton Trans.* **1993**, 2977.
[63] D. M. Dattelbaum, K. M. Omberg, J. R. Schoonover, R. L. Martin, T. J. Meyer, *Inorg. Chem.* **2002**, *41*, 6071.
[64] D. M. Dattelbaum, R. L. Martin, J. R. Schoonover, T. J. Meyer, *J. Phys. Chem. A* **2004**, *108*, 3518.
[65] D. M. Dattelbaum, K. M. Omberg, P. J. Hay, N. L. Gebhart, R. L. Martin, J. R. Schoonover, T. J. Meyer, *J. Phys. Chem. A* **2004**, *108*, 3527.
[66] A. Vlček, Jr., I. R. Farrell, D. J. Liard, P. Matousek, M. Towrie, A. W. Parker, D. C. Grills, M. W. George, *J. Chem. Soc. Dalton Trans.* **2002**, 701.
[67] Apparent decay lifetime of 5.1 ± 0.4 ps was measured at 2062 cm^{-1}. This is a lower limit of the ^{3}MLCT(bpy) population lifetime, since the kinetic measurement is affected by relaxation, whereby the IR band shifts to higher energy with time, and it narrows.
[68] J. K. Hino, L. Della Ciana, W. J. Dressick, B. P. Sullivan, *Inorg. Chem.* **1992**, *31*, 1072.
[69] A. M. Blanco-Rodríguez, M. Towrie, A. Vlček, Jr., unpublished results.
[70] W.-G. Han, T. Lovell, T. Liu, L. Noodleman, *ChemPhysChem* **2002**, *3*, 167.
[71] B. I. Greene, R. M. Hochstrasser, R. B. Weisman, *Chem. Phys. Lett.* **1979**, *62*, 427.
[72] I. K. Lednev, T.-Q. Ye, P. Matousek, M. Towrie, P. Foggi, F. V. R. Neuwahl, S. Umapathy, R. E. Hester, J. N. Moore, *Chem. Phys. Lett.* **1998**, *290*, 68–74.
[73] C.-W. Chang, Y.-C. Lu, T.-T. Wang, E. W.-G. Diau, *J. Am. Chem. Soc.* **2004**, *126*, 10109.
[74] D. D. Perrin, W. L. F. Armarego, *Purification of Laboratory Chemicals*, 3rd ed., Pergamon, Exeter (UK), **1988**.
[75] M. Horner, S. Hünig, *Liebigs Ann. Chem.* **1982**, 1183.
[76] F. W. Vergeer, C. J. Kleverlaan, D. J. Stufkens, *Inorg. Chim. Acta* **2002**, *327*, 126.
[77] P. Matousek, A. W. Parker, P. F. Taday, W. T. Toner, M. Towrie, *Opt. Commun.* **1996**, *127*, 307.
[78] M. Towrie, A. W. Parker, W. Shaikh, P. Matousek, *Meas. Sci. Technol.* **1998**, *9*, 816.
[79] P. Matousek, M. Towrie, A. Stanley, A. W. Parker, *Appl. Spectrosc.* **1999**, *53*, 1485.
[80] P. Matousek, M. Towrie, C. Ma, W. M. Kwok, D. Phillips, W. T. Toner, A. W. Parker, *J. Raman Spectrosc.* **2001**, *32*, 983.
[81] M. Towrie, D. C. Grills, J. Dyer, J. A. Weinstein, P. Matousek, R. Barton, P. D. Bailey, N. Subramaniam, W. M. Kwok, C. S. Ma, D. Phillips, A. W. Parker, M. W. George, *Appl. Spectrosc.* **2003**, *57*, 367.
[82] G. Gritzner, J. Kûta, *J. Pure Appl. Sci.* **1984**, *56*, 461.
[83] F. Hartl, H. Luyten, H. A. Nieuwenhuis, G. C. Schoemaker, *Appl. Spectrosc.* **1994**, *48*, 1522.
[84] T. Mahabiersing, H. Luyten, R. C. Nieuwendam, F. Hartl, *Collect. Czech. Chem. Commun.* **2003**, *68*, 1687.
[85] M. Krejčík, M. Daněk, F. Hartl, *J. Electroanal. Chem. Interfacial Electrochem.* **1991**, *317*, 179.

Received: January 30, 2008
Published online: July 4, 2008

